Huge magneto-optical effects in half-metallic double perovskites

R. Vidya,* P. Ravindran, A. Kjekshus, and H. Fjellvåg
Department of Chemistry, University of Oslo, Box 1033, Blindern, N-0315, Oslo, Norway
(Received 16 July 2004; published 10 November 2004)

Using generalized-gradient-corrected full-potential density-functional calculations we have studied the magneto-optical properties of double perovskites $A_2BB'O_6$, A=Ca, Sr, and Ba; B=Fe; and B'=Mo, W, and Re. Sr_2FeWO_6 has the maximum polar Kerr rotation of 3.87° and specific Faraday rotation of 4.5×10^5 deg cm^{-1}. All other compounds have Kerr rotation more than 1°, except Ca_2FeMoO_6 which has maximum Kerr rotation of 0.5°. Our electronic structure studies show that all these compounds are half-metallic in the ferromagnetic configuration. The large Kerr rotation is found to be due to the combined effects of relatively large exchange splitting from Fe, large spin-orbit coupling due to 4*d* or 5*d* elements, large offdiagonal conductivity, and half-metallicity.

DOI: 10.1103/PhysRevB.70.184414 PACS number(s): 78.20.Ls, 71.20.−b, 78.20.Ci

Materials with large magneto-optical (MO) effects have attracted a lot of attention in both basic and applied research. The motivation stems from desire to develop erasable MO memories and high density disks with MO readout. However, it is still a challenging problem to find a material with large MO rotation and also possessing a collection of necessary magnetic properties.

The interaction of electromagnetic radiation with magnetized matter manifests itself as MO effects. The MO effect due to reflection is called MO Kerr effect (MOKE) and that due to transmission is called MO Faraday effect. Plane-polarized light, when reflected from a metal surface or transmitted through a thin film that has nonzero magnetization will become elliptically polarized with ellipticity (ϵ_K in reflection mode and ϵ_F in transmission mode). The major axis is rotated by the angle θ (θ_K in reflection mode and θ_F in transmission mode) relative to the polarization axis of the incident beam. The MOKE is of three major types, polar, longitudinal, and equatorial. The polar Kerr effect for which the direction of the macroscopic magnetization of the ferromagnetic material and the propagation direction of plane polarized incident beam are perpendicular to the plane of the surface, is the most interesting case and used in practical applications. Digital information, which is suitably stored in a magnetic material can be read out using MOKE. In a transmission mode larger values of the Faraday rotation (θ_F) are clearly an advantage for technological applications.[1]

Transition-metal oxides with ordered double-perovskite structure, $A_2BB'O_6$ (A=Ca, Sr, and Ba; B=Fe, and B'=Mo, W, and Re) have begun to attract the interest of material scientists as magnetoresistive (MR) materials. These compounds are considered as an attractive alternative to the manganese compounds. As MR in manganites is observed near the ferromagnetic transition temperature (T_C), normally below room temperature, it is difficult to fully exploit the potential of manganites.[2]

A lot of efforts have been paid to study the magnetic and MR properties of $A_2BB'O_6$. A majority of these compounds are half-metallic ferromagnets (HMF) or ferrimagnets with T_C in the range of 300–450 K. These compounds also have large perpendicular magnetic anisotropy due to noncubic structure, large magnetic moment on B, large spin-orbit (SO) coupling from B', and various possibilities to substitute the A, B, or B' ions. As they have many of the salient features of potential MO materials, we attempt to study the MO properties of these materials. From full-potential density-functional calculations we show that, in addition to MR applications, $A_2BB'O_6$ can be considered as potential candidates for MO applications. We found good agreement between the calculated and the available experimental MOKE spectra which motivates us to predict MO properties for other compounds in this series. Sr_2FeWO_6 (SFWO) is found to have the maximum polar Kerr rotation ($-3.87°$) and all other compounds have more than 1°, except Ca_2FeMoO_6 (CFMO; $-0.5°$). Interestingly, maximum specific Faraday rotation (θ_F) of all the compounds is found to be more than 1×10^5 deg cm^{-1}. The present work is the first to find such a large MO effect among perovskitelike and double perovskite oxides.

In the ordered double perovskites $A_2BB'O_6$, the transition-metal sites are occupied alternatively by different cations B and B'. Oxygen atoms bridge between B and B', forming alternating octahedra with B or B' as central atom. Owing to the smaller ionic size of Ca^{2+}, alternating FeO_6 and $B'O_6$ (B'=Mo, W and Re) octahedra are tilted considerably, leading to a monoclinic structure (space group $P2_1/n$). Sr_2FeMoO_6 (SFMO) and SFWO are tetragonal with space group $P4_2/n$ and $I4/m$, respectively, whereas Sr_2FeReO_6 (SFRO) is cubic with space group $Fm\bar{3}m$ like other Ba-containing compounds. The monoclinic and tetragonal arrangements have two formula units and the cubic variants have one formula unit per unit cell. For Ca_2FeWO_6 (CFWO), Ba_2FeWO_6 (BFWO), and SFRO, though the crystal structure is known as cubic, explicit structural parameters are not available. Hence we have obtained the optimized structural parameters by force and stress minimization using the projected augmented wave implementation of the Vienna *ab initio* simulation package (VASP).[3] All the studied compounds except SFWO are experimentally found to be ferrimagnetic metals or half-metals with antiparallel spin alignment between Fe and B' moments. SFWO is found to be an antiferromagnetic insulator[4] with $T_N \approx 37$ K. Readers are referred to Refs. 5–10 for a detailed crystal and magnetic structure informations.

The full-potential linear muffin-tin orbital (FPLMTO) calculations[11] presented in this paper are all electron, and no shape approximation to the charge density or potential has been used. The basis set is comprised of augmented linear muffin-tin orbitals.[12] The calculations are based on the generalized-gradient-corrected density-functional theory as proposed by Perdew *et al.*[13] The SO coupling term is included directly in the Hamiltonian matrix elements for the part inside the muffin-tin spheres, hence for spin-polarized cases the size of the secular matrix is doubled. We used a multibasis in order to ensure a well-converged wave function. As experimental polar Kerr rotation is measured by applying an external magnetic field in order to bring about the perpendicular anisotropy, we calculated the MO spectra in the ferromagnetic configuration. For ferromagnetic calculations, the easy magnetization axis is considered along [001]. For the total-energy study the **k**-space integration is done using a minimum of 192 **k** points in the irreducible part of first Brillouin zone (IBZ) and for the optical and MO studies a minimum of 420 **k** points were used in IBZ, depending on the crystal structure.

Because of the metallic nature, a dominant contribution to the optical tensor comes from intraband transitions in the lower-energy region. The intraband contribution to the diagonal components of the conductivity is normally described by the Drude formula,

$$\sigma_D(\omega) = \frac{\omega_p^2}{4\pi\left(\frac{1}{\tau} - i\omega\right)}, \tag{1}$$

where ω_P is the unscreened plasma frequency and τ is the relaxation time which characterizes the scattering of charge carriers, depends on the amount of vacancies and other defects, and therefore varies from sample to sample. Our experience show that if we use τ around 0.3 eV we get good agreement with the experimental spectra. So, we have used τ as a parameter with the value 0.3 eV for all our calculations. The ω_P depends on the concentration of charge carriers. The extraction of Drude parameters from the experimental data requires a free-electronlike region in the optical spectra which does not exist for the compounds studied here. As the experimental determination of Drude parameters is intrinsically difficult, we have chosen an alternative path. We have calculated the spin resolved unscreened plasma frequency by integrating over the Fermi surface using the full-potential linearized augmented plane-wave method as implemented in WIEN2K.[14] The calculations yield the unbroadened absorptive part of the optical conductivity tensor. The interband transitions are affected by scattering events which are phenomenologically described by using a finite lifetime. Since the lifetime of an excited state generally decreases with increased excitation energy, it is relevant and more appropriate to broaden with a function whose width increases with excitation energy. Thus, broadening the calculated optical spectra was performed by convoluting the absorptive optical conductivity with a Lorentzian, whose full width at half maximum (FWHM) was set to 0.01 eV, at photon energy 1 eV. The experimental resolution was simulated by broadening the final spectra with a Gaussian of constant FWHM equal to 0.02 eV. The dispersive parts of the components of the optical conductivity were calculated with a Kramers-Kronig transformation.

With the magnetic moment in the [001] direction of the crystal, the form of the optical conductivity tensor is

$$\sigma = \begin{pmatrix} \sigma_{xx} & \sigma_{xy} & 0 \\ -\sigma_{xy} & \sigma_{xx} & 0 \\ 0 & 0 & \sigma_{zz} \end{pmatrix}. \tag{2}$$

The Kerr rotation (θ_K) and Kerr ellipticity (ϵ_K) can be written as

$$\theta_K + i\epsilon_K = \frac{-\sigma_{xy}}{\sigma_{xx}\sqrt{1 + \frac{4\pi i}{\omega}\sigma_{xx}}}. \tag{3}$$

Similarly, the Faraday rotation (θ_F) and Faraday ellipticity (ϵ_F) are given by,

$$\theta_F + i\epsilon_F = \frac{\omega d}{2c}(n_+ - n_-), \tag{4}$$

where d is the thickness of the film, c is the velocity of light in vacuum, and n_+ and n_- are the refractive indices of the circular waves and given by the eigenvalues of the dielectric tensor. In terms of conductivities they are given as

$$n_\pm^2 = 1 + \frac{4\pi i}{\omega}(\sigma_{xx} \pm i\sigma_{xy}). \tag{5}$$

A detailed description of optical and MO calculation is given in Refs. 15 and 16.

The ferromagnetic calculations of all the compounds converge to be ferrimagnetic, viz., the magnetic moments of Fe and B' are antiparallel to each other. The magnetic moment of Fe is found to be around $3.5\mu_B$ with SFMO having the maximum Fe moment of $3.57\mu_B$. The magnetic moment of B' ranges from -0.1 to $-0.7\mu_B$ with maximum moment possessed by Re ions. The total magnetic moment is nearly an integer, i.e., 3.06 or $3.99\mu_B$/f.u. Our electronic structure studies show that all the compounds are half-metallic (HM) in the ferromagnetic state. They have a small band gap (E_g) in the majority-spin channel and a finite number of states at the Fermi level (E_F) in the minority-spin channel. The magnitude of E_g of all the compounds is given in Table I. The calculated electronic structure and magnetic moments are in good agreement with other ferromagnetic calculations[19,20] for $Sr_2FeB'O_6$, where B'=Mo, W, and Re. The E_g value for SFMO, SFWO, and SFRO is 0.59, 1.36, and 0.56 eV, respectively. The site-projected density of states for the above-mentioned compounds is shown in Fig. 1. In all the three compounds Sr is completely ionized, hence electrons are in the conduction band from 4 to 8 eV. Below E_F, the majority-spin channel is mainly occupied by Fe 3d orbitals and O 2p orbitals. In particular, Fe e_g orbitals are closer to E_F (from -2 to 0 eV) and Fe t_{2g} orbitals are present from -8 to -2 eV with prominent densities from -4 to -2 eV. The B' orbitals are antibonding in the majority-spin channel with t_{2g} orbitals above E_F (from 0.25 to 2 eV) and e_g orbitals are higher-lying (from 4 to 7 eV). The W antibonding t_{2g} orbitals in SFWO are present between 1–2 eV, making its E_g larger

TABLE I. Magnitude of energy gap (E_g) in majority-spin channel, maximum Kerr rotation $\theta_{K\max}$, maximum specific Faraday rotation $\theta_{F\max}$, and maximum figure of merit (FOM; in Kerr configuration) for $A_2FeB'O_6$ (where A=Ca, Sr, and Ba; B'=Mo, W, and Re.) The values in the parenthesis indicate the energy (in eV) at which the maximum occurs.

Composition	E_g(eV)	$\lvert\theta_{K\max}\rvert$(deg)	$\lvert\theta_{F\max}\rvert$($10^5$ deg cm^{-1})	FOM(deg)
Ca_2FeMoO_6	1.02	0.50 (1.25)	1.73 (3.20)	0.23 (2.06)
Ca_2FeWO_6	1.09	1.32 (1.89)	2.28 (1.00)	0.50 (1.90)
Ca_2FeReO_6	0.19	1.04 (1.43)	3.15 (2.48)	0.62 (1.10)
Sr_2FeMoO_6	0.59	1.21 (1.96)	1.04 (1.91)	0.44 (1.92)
Sr_2FeWO_6	1.36	3.87 (1.55)	4.50 (1.48)	1.63 (1.50)
Sr_2FeReO_6	0.56	1.84 (1.72)	3.67 (4.83)	0.90 (1.80)
Ba_2FeMoO_6	0.93	1.46 (0.87)	2.05 (3.25)	0.62 (1.60)
Ba_2FeWO_6	1.80	1.70 (2.83)	4.43 (3.15)	0.69 (2.60)
Ba_2FeReO_6	0.53	1.51 (1.54)	3.10 (2.90)	0.65 (1.54)

compared to the other two compounds, whereas the Re t_{2g} orbitals are just above E_F (from 0.25 to 1.4 eV). In both spin channels O $2p$ orbitals are present from -8 to -2 eV. The B' d orbitals are well hybridized with O $2p$ orbitals so that the bonding states are well-localized (from -8 to -6 eV) and antibonding states are above E_F. The states present at E_F in the minority-spin channel is due to the hybridized Fe and B' t_{2g} orbitals. A more detailed analysis of magnetic and electronic properties will be given elsewhere.[21]

The polar Kerr rotation and Kerr ellipticity spectra for $Ca_2FeB'O_6$, $Sr_2FeB'O_6$, and $Ba_2FeB'O_6$ are given in Figs. 2–4. The peak value of the Kerr rotation for each compound along with the energy at which it occurs is given in Table I.

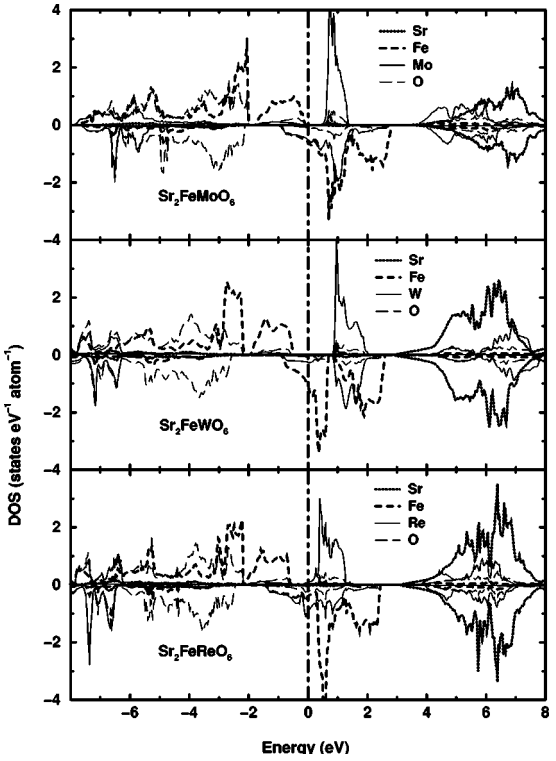

FIG. 1. Site-projected density of states for $Sr_2FeB'O_6$ where B'=Mo, W, and Re.

The calculated Kerr spectra are compared with the available experimental spectra for A_2FeMoO_6 (where A=Ca, Sr, and Ba). The magnitude of the calculated Kerr rotation peaks for CFMO and SFMO agrees very well with that of experiment (at 101 K), but for BFMO theoretical calculations overestimate the magnitude. The position of theoretical MOKE peaks are somewhat shifted in relation to the experimental ones. In general, the peaks of calculated optical conductivities and polar Kerr spectra are displaced toward higher energies with respect to experimental spectra.[16] This may be due to the fact that DFT overestimates the 3d-band width which in turn affects the optical and MO spectra peaks to shift toward higher energy. This can be artificially corrected by increasing lattice parameters which gives narrower bands or

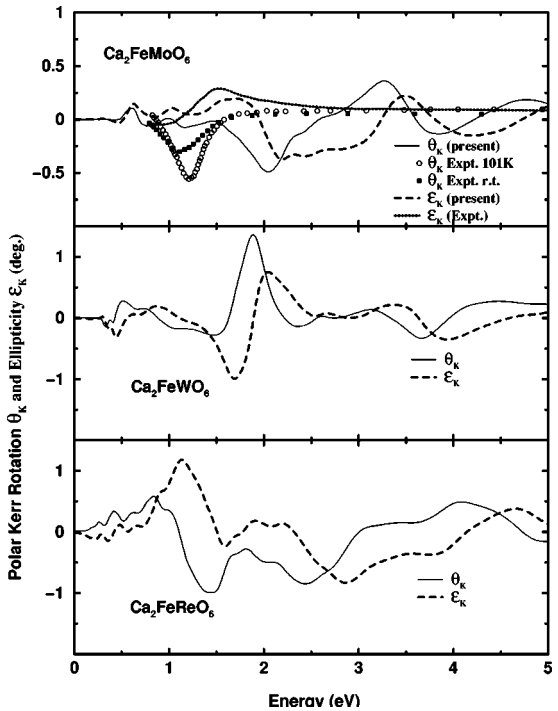

FIG. 2. Polar Kerr rotation (θ_K) and Kerr ellipticity (ϵ_K) spectra for $Ca_2FeB'O_6$ where B'=Mo, W, and Re. Experimental data for CFMO are from Ref. 17.

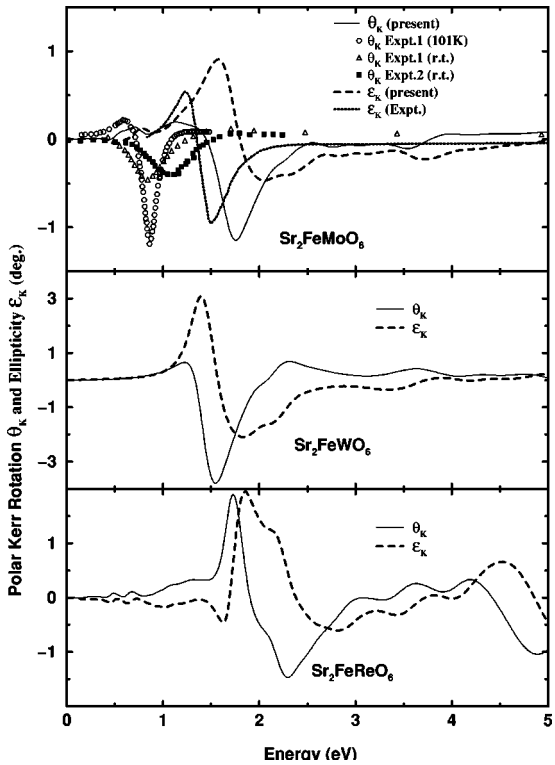

FIG. 3. Polar Kerr rotation (θ_K) and Kerr ellipticity (ϵ_K) spectra for $Sr_2FeB'O_6$ where B'=Mo, W, and Re. Experimental data for SFMO are taken from Ref. 17 (Expt. 1) and Ref. 22 (Expt. 2).

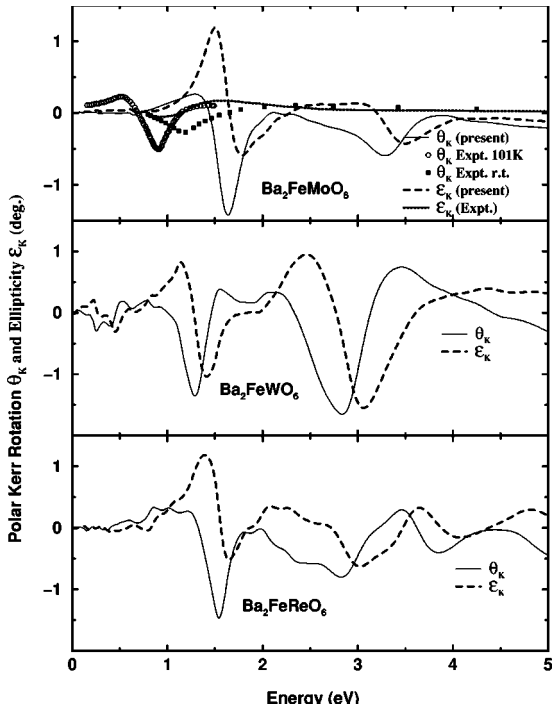

FIG. 4. Polar Kerr rotation (θ_K) and Kerr ellipticity (ϵ_K) spectra for $Ba_2FeB'O_6$ where B'=Mo, W, and Re. Experimental data for BFMO is taken from Ref. 17.

by performing GW-corrected calculations of MO spectra. However, it has to be mentioned that the experimental peak positions are sample-dependent[23] (see for example the Pt-MnSb case in Ref. 24) and appear to depend on stoichiometry, homogeneity, impurities, etc., whereas the magnitude depends on sample preparation, annealing, etc. One month after polishing samples exhibit a marked aging effect compared to the sample just after polishing.[18] The magnitude is enhanced by a factor of 1.5 and the center (or zero-crossing) shifts toward the longer wavelength side.[17] Moreover, we can see that the experimental Kerr rotation peaks for A_2FeMoO_6 are almost doubled at 101 K compared to that at room temperature. It has to be mentioned that we have calculated the MO properties for single crystals at low temperature and hence it is more appropriate to compare our results with the experimental spectra measured at low temperatures for single crystals.

In an attempt to understand the reason for huge MO effects on the studied compounds, we show reflectivity and conductivity spectra for $A_2FeB'O_6$ in Fig. 5. In the top-left panel reflectivities of SFMO, SFWO, and SFRO are shown along with the available experimental spectra for SFMO. Though the essential features of the theoretical spectrum are comparable to that of experimental spectra, the former is shifted by $\sim$0.5 eV toward higher energy region. However, it has to be noted that even the experimental spectrum measured at 10 K is shifted toward higher energy in relation to that measured at 300 K. As mentioned earlier, it would be more appropriate to compare our theoretical spectra with experimental spectra at low temperature. Moreover, the reflectivity spectra exhibit remarkable aging effects due to oxidation of the surface of the samples (similar to Kerr spectra). The amplitude of reflectivity for the sample just after polishing is more than two times larger than that of the sample one month after polishing (as seen in the experimental spectra for SFMO in Fig. 5). A dip in the reflectivity spectra in the lower energy region (around 1.7 eV) has been experimentally interpreted as due to the plasma resonance of conduction electrons in the crystal since the diagonal and offdiagonal elements of the dielectric tensor is expected to exhibit an anomaly near the plasma edge.[25] Therefore both reflectivity and Kerr spectra are affected by this. In order to check whether the dip around 1.7 eV is really due to plasma resonance, we have also calculated the electron energy loss spectrum (EELS). The function representing characteristic energy losses (or plasmon oscillations) is proportional to the probability that a fast electron moving across a medium loses energy per unit length. Generally speaking, plasma resonances manifest themselves as rather distinct peaks in the EELS,[26] and are thus a feature easily observed experimentally. The EELS for SFMO, SFWO, and SFRO show prominent peaks at 1.62, 1.49, and 1.14 eV, respectively. The reflectivity spectra of SFWO and SFRO also show a dip at 1.3 and 1.6 eV, respectively. Hence, the dip observed in these compounds is due to the plasma resonance. However, no experimental reflectivity spectra are available for SFWO and SFRO to compare our theoretical spectra with. As Kerr spectra show peaks for all these compounds in the energy region 1–2 eV, plasma resonance also plays an important role in the θ_{Kmax} values (Fig. 5).

The real part of diagonal conductivity of SFMO is in reasonable agreement with the available experimental spectra,

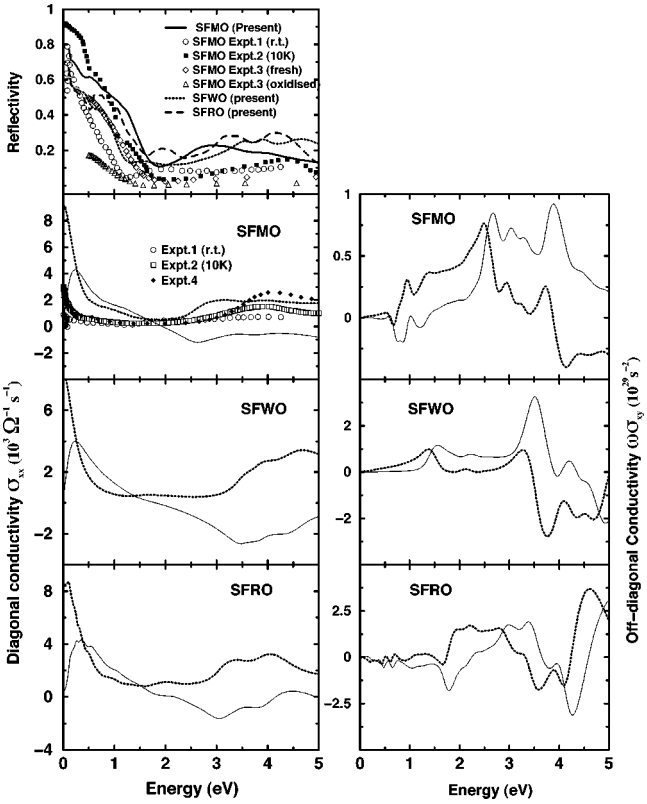

FIG. 5. Reflectivity and conductivity spectra for $Sra_2FeB'O_6$ where B' = Mo W, and Re. Experimental data for SFMO are taken from Ref. 27 (Expt. 1), Ref. 28, (Expt. 2), Ref. 18 (Expt. 3), and Ref. 29 (Expt. 4).

except that the amplitude of theoretical spectra is higher than that of experimental spectrum in the lower energy region. As experimental spectra are derived through Kramers-Kronig transformation of reflectivity spectra, there is slight discrepancy. The Drude component is involved in the theoretical conductivities, which will enhance the amplitude in the lower energy region. Around 0.5 eV, a small bump is observed which is due to Fe $e_g^{\uparrow}$ to Mo $t_{2g}^{\uparrow}$ transition. The peak at 4 eV observed by experiments is shifted to 3 eV, instead a small bump is seen at 4 eV. This peak is attributed to the O $2p$ to hybridized $t_{2g}^{\downarrow}$ of Fe and Mo. In the case of SFWO, two prominent peaks occur around 4 and 4.5 eV. The first peak is due to O $2p$ to Fe $t_{2g}^{\downarrow}$ transition and the second peak is due to O $2p$ to W $t_{2g}^{\uparrow}$ transition. Around five peak structures appear for SFRO. An experimental study[30] is available for this compound up to 0.8 eV. However, no prominent structure exists within that narrow energy region to be compared with our theoretical spectrum. The lower energy peaks at 0.6 and 0.8 eV can be attributed to the interband (Fe $e_g^{\uparrow}$ to Re $t_{2g}^{\uparrow}$) transition. The peaks at 2 and 3.25 eV are due to O $2p$ to Fe and Re hybridized $t_{2g}^{\downarrow}$ transition. The peak around 4 eV is due to O $2p$ to $t_{2g}^{\uparrow}$ transition. From the figure it can be seen that the overall topology of the diagonal conductivity for the three compounds is somewhat similar. As experimentalists often display $\omega\sigma_{xy}$ instead of σ_{xy}, we also show $\omega\sigma_{xy}$ in the right panel of Fig. 5. From Eq. (3) it can be seen that the Kerr rotation can be enhanced by a larger off-diagonal conductivity and a smaller diagonal conductivity. The diagonal conductivity of all three compounds shows a minimum around 1.5–2 eV where maximum of θ_K is observed. The off-diagonal conductivity of SFWO and SFRO show higher values than that of SFMO, implying that the high Kerr rotation of these compounds also result from high off-diagonal conductivity. The influence of intraband effects on the MOKE is restricted to energies smaller than 1–2 eV.

The MOKE signal is proportional to $f \cdot M$, where f is determined by the complex refractive index at the probe frequency and M is the magnetization.[22] The refractive index of SFMO, SFWO, and SFRO in the energy region 1–2 eV (where $\theta_{K\max}$ occurs) is 1.56, 1.88, and 1.98, respectively. Though the refractive index of SFWO is slightly smaller than SFRO, its magnetic moment is $3.99\mu_B$ whereas SFRO has $3.07\mu_B$. So it has larger $\theta_{K\max}$ than SFMO and SFRO. The fact that the Kerr rotation correlates with the atomic magnetic moment of spin should not be surprising since the MO effect involves spin-orbit interaction.[31] Incident photons excite the $3d$ valence electrons of the transition metals by altering their orbital angular momenta. When the electrons fall back from their excited states, the emitted photons are polarized and characteristic of both spin orientation and magnitude. Thus, the SO interaction couples the momentum of the electron with its spin and provides the link for the circularly-polarized electromagnetic waves to couple to the magnetization of the material. The heavier the atom, the stronger will be the SO interaction. Thus, all the studied compounds have large MO effects. Moreover, SFWO has maximum exchange splitting of 3.1 eV and its band gap in the majority spin channel is 1.36 eV. So the electrons are highly spin polarized in the HMF state. Therefore, larger off-diagonal conductivity, refractive index, magnetic moment, SO coupling, exchange splitting, band gap, and plasma resonance combine to give huge MO values for all the studied compounds, and in particular to SFWO. The polar Kerr ellipticity is a measure of how the shape of the wave has changed upon reflection and depends only on the absolute magnitudes of the reflection coefficients. As the reflectivities of these compounds are also large, they also have large polar Kerr ellipticity.

The Kerr rotation peaks of all the studied compounds lie in the energy region of infrared to visible radiation. An intense search is going on for materials with MO peaks in the lower wavelength region for use in high-density storage.[1] Among the studied compounds CFRO (−0.89° at 2.47 eV), SFRO (−1.5° at 2.3 eV), BFWO (−1.70° at 2.83 eV), and BFRO (−0.86° at 2.83 eV) have large peaks in the green-violet energy region. It has to be noted that a large polar Kerr rotation, typically greater than about 0.2° is clearly of benefit in reading information stored in a thermo-MO thin film.[1] The strong SO coupling results in a large uniaxial anisotropy which is one of the essential requirements for a MO storage device. The magnitude of the uniaxial anisotropy depends on structural anisotropy and hence noncubic systems usually possess large magnetic anisotropy. Moreover flexibility to substitute or dope A, B or B' elements will be useful to tune the MO properties according to the need. In that perspective the present compounds may be of relevance for high-density storage applications.

In a transmission mode, large Faraday rotation is desirable for applications.[32] Materials with large Faraday rotation are

used in devices called optical isolators.[33] Therefore we predict the specific Faraday rotation and ellipticity of $A_2FeB'O_6$ (not shown), experimental Faraday spectra are hitherto not available for comparison. In Table I we have given the maximum of specific Faraday rotation for each compound. Specific Faraday rotation of all the studied compounds is greater than 1×10^5 deg cm^{-1}. It is interesting to note that SFWO has the maximum Kerr as well as Faraday rotation among $A_2FeB'O_6$.

In order to detect the written information in a MO medium easily, and to make the signal-to-noise ratio as high as possible, the MO figure of merit (FOM) should be large.[1] FOM is defined[34] as FOM$\approx\sqrt{R(\theta_K^2+\epsilon_K^2)}$, where R, is reflectivity and θ_K and ϵ_K as defined earlier. For the sake of simplicity, in Table I we have given the maximum of FOM and the corresponding energy at which it occurs. The FOM calculated for the present compounds is comparable with that of the well-known MO material PtMnSb. In spite of the fact that FOM is often used to characterize the performance of a MO medium and the factors determining FOM depend on the structure on which magnetic material is embedded, we believe that the given large FOM values may motivate more MO studies on these systems.

In conclusion, the presently studied compounds have many of the basic requirements[35] for a MO medium, such as presence of uniaxial magnetic anisotropy, T_C ranging between 300 and 600 K, large Kerr rotation, large Faraday rotation, large FOM, HMF at room temperature, long term stability, etc. For the first time, using full-potential density functional calculations, we have shown that $A_2BB'O_6$ have the huge MO effects among the oxides and can be considered as potential candidates for MO applications. The huge magneto-optical effects are found to result due to combined effects of large off-diagonal conductivity, refractive index, magnetic moment, SO coupling, exchange splitting, band gap, and plasma resonance.

The authors are grateful to the Research Council of Norway for financial support and computer time at the Norwegian supercomputer facilities. R.V. and P.R. wish to acknowledge Dr. J. Wills and Dr. A. Delin for providing the computer programs used in this study, and Professor Claudia Ambrosch-Draxl and Dr. S. Sharma for useful discussions.

*Electronic address: vidya.ravindran@kjemi.uio.no

[1] P.J. Grundy, in *Electronic and Magnetic Properties of Metals and Ceramics*, Materials Science and Technology, edited by K.H.J. Buschow (VCH, FRG, 1994), Vol. 3B, p. 575.
[2] O. Chmaissem, R. Kruk, B. Dabrowski, D.E. Brown, X. Xiong, S. Kolesnik, J.D. Jorgensen, and C.W. Kimball, Phys. Rev. B **62**, 14 197 (2000).
[3] G. Kresse and J. Hafner, Phys. Rev. B **47**, 558 (1993); G. Kresse and J. Furthmuller, Comput. Mater. Sci. **6**, 15 (1996).
[4] G. Blasse, Philips Res. Rep. **20**, 327 (1965); H. Kawanaka, I. Hase, S. Toyoma, and Y. Nishihara, J. Phys. Soc. Jpn. **68**, 2890 (1999).
[5] K.-I. Kobayashi, T. Kimura, H. Sawada, K. Terakura, and Y. Tokura, Nature (London) **395**, 677 (1998).
[6] C. Ritter, M.R. Ibarra, L. Morellon, J. Blasco, and J.M. De Teresa, J. Phys.: Condens. Matter **12**, 8295 (2000).
[7] J. Gopalakrishnan, A. Chattopadhyay, S.B. Ogale, T. Venkatesan, R.L. Greene, A.J. Millis, K. Ramesha, B. Hannoyer, and G. Marest, Phys. Rev. B **62**, 9538 (2000).
[8] Y. Moritomo, S. Xu, A. Machida, T. Akimoto, E. Nishibori, M. Takata, M. Sakata, and K. Ohoyama, J. Phys. Soc. Jpn. **69**, 1723 (2000).
[9] W. Prellier, V. Smolyaninova, A. Biswas, C. Galley, R.L. Greene, K. Ramesha, and J. Gopalakrishanan, J. Phys.: Condens. Matter **12**, 965 (2000).
[10] L. Pinsard-Gaudart, R. Suryanarayanan, A. Revcolevschi, J. Rodriguez-Carvajal, J.-M. Greneche, P.A.I. Smith, R.M. Thomas, R.P. Borges, and J.M.D. Coey, J. Appl. Phys. **87**, 7118 (2000).
[11] J.M. Wills, O. Eriksson, M. Alouani, and D.L. Price, in *Electronic Structure and Physical Properties of Materials*, edited by H. Dreysse (Springer, Berlin, 2000), p. 148.
[12] O.K. Andersen, Phys. Rev. B **12**, 3060 (1975).
[13] J.P. Perdew, K. Burke, and M. Ernzerhof, Phys. Rev. Lett. **77**, 3865 (1996).
[14] P. Blaha, K. Schwarz, G.K.H. Madsen, D. Kvasnicka, and J. Luitz, WIEN2k, revised edition, 2001.
[15] P. Ravindran, A. Delin, P. James, B. Johansson, J.M. Wills, R. Ahuja, and O. Eriksson, Phys. Rev. B **59**, 15 680 (1999).
[16] A. Delin, O. Eriksson, B. Johansson, S. Auluck, and J.M. Wills, Phys. Rev. B **60**, 14 105 (1999).
[17] K. Shono, M. Abe, M. Gomi, and S. Nomura, Jpn. J. Appl. Phys., Part 1 **21**, 1720 (1982).
[18] K. Shono, M. Abe, M. Gomi, and S. Nomura, Jpn. J. Appl. Phys. **20**, L426 (1981).
[19] I.V. Solevyev, Phys. Rev. B **65**, 144446 (2002).
[20] Z. Fang, K. Terakura, and J. Kanamori, Phys. Rev. B **63**, 180407 (2001).
[21] R. Vidya, P. Ravindran, H. Fjellvåg, and A. Kjekshus (unpublished).
[22] T. Kise, T. Ogasawara, M. Ashida, Y. Tomioka, Y. Tokura, and M. Kuwata-Gonokami, Phys. Rev. Lett. **85**, 1986 (2000).
[23] U. Rüdiger, M. Rabe, G. Güntherodt, H.Q. Yin, R.I. Dass, and J.B. Goodeneough, Appl. Phys. Lett. **77**, 2216 (2000).
[24] K. Takanashi, K. Sato, J. Watanabe, Y. Sato, and H. Fujimori, Jpn. J. Appl. Phys., Part 1 **30**, 52 (1991).
[25] G. Dresselhaus, A.F. Kip, and C. Kittel, Phys. Rev. **100**, 618 (1955).
[26] P. Ravindran, A. Delin, R. Ahuja, B. Johansson, S. Auluck, J.M. Wills, and O. Eriksson, Phys. Rev. B **56**, 6851 (1997).
[27] Y. Moritomo, S. Xu, A. Machida, T. Akimoto, E. Nishibori, M. Takata, and M. Sakata, Phys. Rev. B **61**, R7827 (2000).
[28] Y. Tomioka, T. Okuda, Y. Okimoto, R. Kumai, K.-I. Kobayashi, and Y. Tokura, Phys. Rev. B **61**, 422 (2000).
[29] J.H. Jung, S.-J. Oh, M.W. Kim, T.W. Noh, J.-Y. Kim, J.-H. Park, H.-J. Lin, C.T. Chen, and Y. Moritomo, Phys. Rev. B **66**,

104415 (2002).
[30] H. Kato, T. Okuda, Y. Okimoto, Y. Tomioka, K. Oikawa, T. Kamiyama, and Y. Tokura, Phys. Rev. B **65**, 144404 (2002).
[31] P.M. Oppeneer, T. Maurer, J. Sticht, and J. Kübler, Phys. Rev. B **45**, 10 924 (1992).
[32] J. Schones, in *Electronic and Magnetic Properties of Metals and Ceramics*, Materials Science and Technology, edited by K.H.J. Buschow (VCH, FRG, 1994), Vol. 3B, p. 233.
[33] D.K. Wilson, Mater. Res. Soc. Symp. Proc. **517**, 541 (1998).
[34] M. Mansuripur, *The Physical Principles of Magneto-Optical Recording* (Cambridge University Press, Cambridge, 1995), p. 206.
[35] P. Hansen, J. Magn. Magn. Mater. **83**, 6 (1990).